IAEA-SM-174/60

LA-UR - 73-972

Conf- 730823--3

TITLE: Calculation of Fission Barriers for Heavy Neutron-Rich Nuclei

AUTHOR(S): W. M. Howard and J. R. Nix

SUBMITTED TO: For Presentation at the Third IAEA Symposium on the Physics and Chemistry of Fission, Rochester, New York, August 13-17, 1973

los alamos scientific laboratory
of the University of California
LOS ALAMOS, NEW MEXICO 87544

Form No. 836
St. No. 2629
1/73

UNITED STATES
ATOMIC ENERGY COMMISSION
CONTRACT W-7405-ENG. 36

MASTER

CALCULATION OF FISSION BARRIERS FOR HEAVY NEUTRON-RICH NUCLEI*

W. M. Howard and J. R. Nix
Los Alamos Scientific Laboratory, University of California
Los Alamos, New Mexico, United States of America

ABSTRACT

We study the possible production of superheavy nuclei by the multiple capture of neutrons in the astrophysical r-process, the conventional thermonuclear explosion, and the multistep explosions proposed by Meldner. This is done by calculating the fission barriers and neutron separation energies for the appropriate region of heavy neutron-rich nuclei. We use an improved version of the macroscopic-microscopic method. The macroscopic energy is calculated according to the droplet model of Myers and Swiatecki, with constants they determined in January 1973 by adjustments to experimental nuclear ground-state masses and fission-barrier heights and from statistical calculations. The microscopic corrections to the energy are calculated from a diffuse-surface single-particle potential of the folded Yukawa type. The potential radius is taken from the statistical calculations of Myers; the potential well depths and diffuseness and the spin-orbit interaction strengths are adjusted to reproduce experimental single-particle levels in heavy nuclei.

The calculated fission barriers are displayed as functions of the distance between the centers of mass of the two nascent fragments. The actual shapes considered are the sequence of idealized liquid-drop-model saddle-point shapes (the so-called y family of shapes) for distortions up to the vicinity of the saddle point. For larger distortions the most probable idealized liquid-drop-model dynamical path is used. The neutron separation energies are calculated from ground-state masses that are determined by minimizing the potential energy with respect to the nuclear quadrupole moment Q_2 and hexadecapole moment Q_4.

For a broad region of heavy neutron-rich nuclei the calculated fission barriers are less than the calculated neutron separation energies. This stems primarily from the predicted rapid decrease in the effective surface tension of a nucleus with increasing neutron excess. Therefore, the capture of a neutron should excite the nucleus above the top of the fission barrier and consequently terminate the neutron-capture process before any superheavy nuclei are produced.

*Work performed under the auspices of the U. S. Atomic Energy Commission.

1. INTRODUCTION

The prediction of the possible existence of superheavy nuclei has led to attempts to produce them in the laboratory and to searches for them in nature. Calculations of the nuclear properties of such nuclei by Myers and Swiatecki [1], Nilsson and his coworkers [2], and more recently by other workers [3,4] have predicted half-lives as long as 10^9 yr. Thus, if these nuclei are produced in astrophysical environments, they should be detectable on the earth and in the cosmic rays impinging on the earth. Thus far, efforts to produce superheavy nuclei in the laboratory or to find them in nature have failed.

In this paper, we study the effectiveness of the mechanism that nature would use to produce them as well as the mechanism that man might use if he employed nuclear explosions. In particular, we study the astrophysical r-process, the conventional thermonuclear explosion, and the multistep process proposed by Meldner [5]. Neutron-induced fission plays the critical role in terminating these processes; we therefore calculate the fission barriers and neutron separation energies for a broad region of heavy neutron-rich nuclei.

Figure 1 is a plot of known and predicted nuclei as a function of the neutron number N and proton number Z. The heaviest points represent stable nuclei, the medium-size points nuclei with half-lives greater than one year, and the lightest points nuclei with half-lives less than one year. Nuclei with predicted half-lives greater than about five minutes are included in the island of superheavy nuclei [4]. The dashed lines outline the region of nuclei where we calculate fission barriers and nuclear ground-state masses. Our fission-barrier calculations are limited to even nuclei. The solid lines indicate the approximate regions of heavy neutron-rich nuclei through which the various processes occur.

In Sec. 2 we discuss the method of calculation, in Sec. 3 our results, in Sec. 4 the significance of our results to these various neutron-capture processes, and in Sec. 5 our conclusions.

2. METHOD OF CALCULATION

The potential energy surfaces for these heavy neutron-rich nuclei are calculated by use of the macroscopic-microscopic method as described in the previous review paper on the calculation of fission barriers [6]. The macroscopic energy is calculated according to the droplet model of Myers and Swiatecki [7,8], with constants they determined in January 1973 by adjustments to experimental nuclear ground-state masses and fission-barrier heights and from statistical calculations. The droplet model takes into account terms of order $A^{1/3}$ in the nuclear energy as well as a more precise dependence of the effective surface energy on the neutron excess. The microscopic corrections to the energy are calculated from a diffuse-surface single-particle potential of the folded Yukawa type. The potential radius is taken from the statistical calculations of Myers [9]; the potential well depths are adjusted to reproduce experimental single-particle levels in heavy spherical nuclei and the diffuseness and spin-orbit interaction strengths in heavy deformed nuclei [6]. This macroscopic-microscopic method is consistent with experimental fission barriers and ground-state masses in the actinide region as well as with information from conventional nuclear explosions in the neutron-rich region.

The neutron separation energies are calculated from ground-state masses that are determined by minimizing the potential energy with respect to the nuclear quadrupole moment Q_2 and the hexadecapole moment Q_4. The nuclear shapes are described in terms of smoothly joined portions of three quadratic surfaces of revolution [10,11]. One of the three symmetric coordinates that define such shapes is eliminated by requiring that the relative quadrupole moment of the middle spheroid be equal in magnitude but of opposite sign to the relative quadrupole moment of either end spheroid. The two remaining coordinates are chosen to be the quadrupole moment Q_2 and hexadecapole moment Q_4 of the shape.

For the droplet-model mass excess we use the following form [7,8], where it is understood that all energies and masses are in MeV and that all lengths are in fm:

$$\begin{aligned} M(Z,A;\ \text{shape}) = {} & 8.07169\ (A-Z) + 7.28922\ Z \\ & + (-\ a_1 + J\bar{\delta}^2 - \tfrac{1}{2}K\bar{\epsilon}^2 + \tfrac{1}{2}M\bar{\delta}^4)\ A \\ & + (a_2 + \tfrac{9}{4}[\tfrac{J^2}{Q}]\bar{\delta}^2)\ A^{2/3}B_s \\ & + a_3A^{1/3}B_k + C_1Z^2A^{-1/3}B_c - C_2Z^2A^{1/3}B_r \\ & - C_3Z^2A^{-1} - 2^{-1/3}C_4Z - C_5Z^2B_w \\ & + 30|I| + \tfrac{11}{\sqrt{A}}\delta' + \tfrac{30}{A}\delta'' \quad , \end{aligned} \tag{1}$$

where

$$I = \frac{A-2Z}{A} \quad , \tag{2}$$

$$\bar{\delta} = \frac{\left(I + \frac{3}{16}[\frac{C_1}{Q}]ZA^{-2/3}B_v\right)}{\left(1 + \frac{9}{4}[\frac{J}{Q}]A^{-1/3}B_s\right)} \quad , \tag{3}$$

$$\bar{\epsilon} = (-\ 2a_2A^{-1/3}B_s + L\bar{\delta}^2 + C_1Z^2A^{-4/3}B_c)/K \quad , \tag{4}$$

$$C_1 = \frac{3}{5}\frac{e^2}{r_0} \quad , \tag{5}$$

$$C_2 = \frac{C_1{}^2}{168}\left(\frac{1}{2J} + \frac{9}{K}\right) \quad , \tag{6}$$

$$C_3 = \frac{5}{2}C_1\left(\frac{b}{r_0}\right)^2 \quad , \tag{7}$$

$$C_4 = \frac{5}{4}\left(\frac{3}{2\pi}\right)^{2/3} C_1 \quad , \tag{8}$$

$$C_5 = \frac{C_1^{\,2}}{64Q} \quad , \tag{9}$$

$$\delta' = \begin{cases} +1, & \text{odd nuclei} \\ 0, & \text{odd-particle nuclei} \\ -1, & \text{even nuclei} \end{cases} \quad , \tag{10}$$

$$\delta'' = \begin{cases} 1, & \text{even nuclei with } A = 2Z \\ 0, & \text{otherwise} \end{cases} \quad . \tag{11}$$

The six relative energies B_i are functions only of the nuclear shape and are defined so as to have the value unity for a sphere. The quantities B_s and B_c are the relative surface and coulomb energies of the liquid-drop model, B_k is the relative curvature energy, B_r is the relative coulomb redistribution energy in the nuclear volume, and B_v and B_w are two types of relative coulomb redistribution energy in the nuclear surface. The reader is referred to Ref. [7] for the relevant equations to calculate these shape-dependent terms. From a combination of statistical calculations and adjustments to nuclear ground-state masses and fission-barrier heights, values for the constants that appear are determined to be [8]: $a_1 = 15.986$, $a_2 = 20.760$, $a_3 = 0$, $J = 36.5$, $Q = 17$, $r_0 = 1.175$, $K = 240$, $L = 100$, $M = 0$, and $H = 0.99$. Notice that the coefficient of the curvature term is identically zero. The difference in Eq. (1) relative to what appears in Ref. [7] for the coulomb term multiplying C_4 arises because the substitution $A = 2Z$ has been made.

There is much interest in the value of the surface-asymmetry constant κ in liquid-drop-model mass formulas because it has an important bearing on the fissility of neutron-rich nuclei. In the droplet-model the shape dependence of the potential energy is more complicated than in the liquid-drop model, and the constant κ no longer enters. However, by neglecting the relatively small influence of the four new shape-dependent energies, the more complicated dependence of the droplet model on the surface and coulomb energies can be described approximately in terms of an effective value of κ which would yield the same saddle point as the liquid-drop model [12]. The result is

$$\kappa_{eff} = \frac{\frac{9}{4}\left(\frac{J^2}{Q}\right)}{a_2\left(1 + \frac{9J\hat{B}_s}{4QA^{1/3}}\right)^2} \quad , \tag{12}$$

where $\hat{B}_s$ is the relative surface energy of the saddle-point shape. Thus, unlike in the liquid-drop model, this effective value of κ depends on the mass number and the saddle-point shape. For the neutron-rich nucleus ^{280}Pu, where the macroscopic saddle-point shape is close to $y = 0.10$, we obtain $\kappa_{eff} = 2.8$. This is significantly higher than the frequently used value of $\kappa = 1.7826$ in the liquid-drop model [13]. Thus, in the droplet model the effective surface tension decreases much more rapidly with neutron excess than in the liquid-drop model of Myers and Swiatecki.

The fission barriers are calculated for the sequence of idealized liquid-drop-model saddle-point shapes (the so-called y family of shapes) for distortions up to the vicinity of the saddle point. For larger distortions we use the most probable idealized liquid-drop-model dynamical path [10,11]. The barrier heights that we calculate should be considered upper limits since we have not included mass-asymmetric or axially asymmetric (γ) distortions. As shown in the previous paper [6] inclusion of these effects could lower our calculated barriers by 1 or 2 MeV.

3. RESULTS OF CALCULATION

Figure 2 is a comparison of the experimental ground-state single-particle correction for nuclei in the lead, rare-earth, and actinide regions with our calculated values. The discrepancies oscillate with particle number and are as large as 4 MeV for nuclei close to ^{226}Th. Part of the error for these nuclei arises because the constrained version of the three-quadratic-surface parametrization that we are using does not describe adequately shapes with large positive hexadecapole moments: the generated shapes have a large curvature near the equator, which increases substantially the surface energy. The error for these nuclei can be reduced (by up to 1.2 MeV for ^{226}Th) by use [6] of the coordinates ε and ε_4 in Nilsson's perturbed-spheroid parametrization [2]. However, for several nuclei with neutron number N close to 152, the energy calculated by use of the coordinates Q_2 and Q_4 is lower (by up to 0.4 MeV for ^{252}Cf). Comparing this figure with the results of Ref. [6], different conventions are adopted here concerning two separate points. First, our calculated values do not include any zero-point energy. Second, they are relative to the pairing convention of Myers and Swiatecki [8,13], in which an odd-particle nucleus rather than an even nucleus has zero pairing energy. The combined effects of these two differences increase our calculated values by 0.2 to 0.3 MeV relative to those in Ref. [6].

Figures 3, 4, and 5 show some of our calculated barriers as functions of the distance between the centers of mass of the two nascent fragments. We note that the droplet-model contribution to the potential energy is greatly reduced for an increased neutron excess; this is because the effective surface-asymmetry constant for these nuclei is relatively large ($\kappa_{eff} = 2.8$). The barriers are also greatly reduced with increasing proton number due to the strong dependence of the fissility on the disruptive coulomb force. The large second peaks on the barriers of ^{248}U, ^{252}U, and ^{256}U should be reduced by at least 1 or 2 MeV when mass-asymmetric distortions are taken into account.

Our calculated barriers for superheavy nuclei are displayed in Fig. 5; they are very similar to those calculated by Bolsterli et al. [3]. There are three differences in those two calculations: (1) we employ the full droplet model for the macroscopic energy instead of the liquid-drop model, (2) we adjust the surface diffuseness and the spin-orbit interaction strengths to reproduce experimental single-particle levels in the rare-earth and actinide nuclei instead of in ^{208}Pb, and (3) beyond the vicinity of the saddle point we use the liquid-drop-model dynamical path instead of the y-family sequence of shapes.

The barriers for ^{294}118, ^{298}118, ^{302}118, ^{290}114, ^{294}114, and ^{298}114 are all over 10 MeV high. The barrier for ^{298}114 is slightly lower than in the previous calculation [3,4]; however, in our calculation the barriers for $^{294}114$ and $^{298}118$ (at N = 180) are larger than the barriers for $^{298}114$ and $^{302}118$ (at N = 184). As in the previous calculations, when neutrons are added beyond N = 184, the barrier height decreases drmatically. We predict the superheavy island to be somewhat more stable in the neutron-deficient direction than has been predicted by previous calculations. This is due to the increased spin-orbit interaction strengths and the decreased surface-diffuseness parameter [6] that we use. This change has the effect of decreasing the neutron level density below N = 180, which increases the binding of nuclei with neutron numbers near N = 180.

Figure 6 is a contour plot of the calculated fission-barrier height for even nuclei. We include a zero-point energy of 0.5 MeV for motion in the fission direction. Figure 7 is a contour plot of the calculated neutron separation energy for even nuclei, and Fig. 8 is a contour plot of the difference between the calculated fission-barrier height and the calculated neutron separation energy for even nuclei. We will employ these three figures in evaluating where neutron-induced fission will terminate the various multiple-neutron-capture processes. We have not performed any spontaneous-fission half-life calculations.

4. APPLICATION OF RESULTS TO MULTIPLE-NEUTRON-CAPTURE PROCESSES

4.1 Astrophysical r-process

The astrophysical r-process [14] is the multiple capture of neutrons on heavy nuclei on a time scale that is much shorter than beta-decay half-lives for heavy neutron-rich nuclei. In some catastrophic supernova events the high-density matter is thermalized to an energy of order 200 keV, so that neutron capture is impeded by neutron photodisintegration at a low neutron separation energy. The neutron-capture flow thus proceeds far to the neutron-rich side of the valley of beta stability. Neutron separation energies decrease dramatically immediately after a closed shell of neutrons, which tends to halt temporarily the capture flow. When beta decays increase the proton number sufficiently, neutron separation energies again become large enough to allow the capture flow to continue. Figure 1 shows a typical r-process capture path. Since the nuclei along the path are in statistical equilibrium with respect to the exchange of photons and neutrons, the r-process path is determined by the neutron separation energies of the neutron-rich nuclei and, in fact, follows a path of essentially constant neutron separation energy.

There has been much interest as to whether superheavy nuclei can be produced in the r-process, which is known to produce many of the naturally occurring neutron-rich nuclei between germanium and bismuth and all of the naturally occurring nuclei heavier than bismuth. Two groups [15,16] have studied in some detail the fission properties of heavy neutron-rich nuclei in regard to the production of superheavy nuclei by use of the macroscopic-microscopic approach. Boleu et al. [15] have calculated the nuclear potential-energy surface with the modified harmonic-oscillator potential and the liquid-drop model of Myers and Swiatecki [13]. They conclude that even with a low surface asymmetry constant (κ = 1.7826) superheavy nuclei cannot be produced by the conventional r-process. They find that the r-process would be terminated by neutron-induced fission at approximately Z = 98 and N = 186. However, these calculations are performed with a pairing strength proportional to the surface area, which reduces the barrier with increasing distortion. According to Ref. [4], the lightest superheavy nucleus with an astrophysically significant half-life is A = 291 (Z = 110, N = 181).

Schramm and Fiset [16] also use the Myers and Swiatecki [13] liquid-drop model for the macroscopic contribution to their barriers and the diffuse-surface single-particle potential of the folded Yukawa type [3] for the microscopic corrections to the energy. In addition, they studied the dependence of the results on the value of the surface-asymmetry constant κ. The neutron separation energies were calculated from the 1966 mass formula of Myers and Swiatecki [1], which included am empirical microscopic-energy correction. However, their neutron spearation energies are similar to those that we calculate. They predict the neutron-induced-fission cutoff to be near $Z = 100$ and $N = 190$ (for $\kappa = 1.7826$). Since the Myers-Swiatecki mass formula predicts a broad r-process path, material below the neutron-induced-fission cutoff but with higher mass number A survives. By carefully following the decay back to the superheavy island they find that significant amounts of nuclei with $A = 290$, 291, 292, and 293 survives, depending on what is included for the zero-point energy.

For a given determination of the neutron separation energy for neutron-rich nuclei, the r-process path can be determined approximately without carrying out a full r-process calculation. When calculating neutron-induced fission on the approach to the superheavy island, it is important to know where the r-process path will occur in this region.

There exist two peaks in the solar system abundance distribution of r-process nuclei, at $A = 130$ and $A = 195$. These peaks are due to an accumulation of material along the r-process path at the neutron closed shells $N = 82$ and $N = 126$. The second peak extends through the region $185 \lesssim A \lesssim 200$; the r-process path must therefore pass through the same mass region at $N = 126$. The neutron separation energies in the region where the path enters and leaves the neutron-closed shell at $N = 126$ therefore determines the values of the neutron separation energy that the r-process path follows.

We calculate the neutron separation energies in this region to be $B_n = 3 \pm 1$ MeV. We therefore find from a study of Figs. 7 and 8 that the neutron-induced-fission cutoff is $Z = 96$ and $N = 186$; this is somewhat lower than the estimates by Boleu et al. [15] and Schramm and Fiset [16].

Thus, we predict that nuclei with mass number $A = 281$ will be the last to survive in the r-process before neutron-induced fission terminates the path. According to the results of Ref. [4], nuclei with mass number 281 would spontaneously fission with half-lives of the order of 1 sec after a few beta decays. In order for superheavy nuclei to be observed in cosmic rays, their half-lives would need to be at least 10^6 yr. This would require the production of nuclei with mass number $A \gtrsim 291$, which is 10 mass units higher than the heaviest yield that we predict. This lower neutron-induced-fission cutoff is due primarily to the rapid decrease predicted by the droplet model of the surface energy with the addition of neutrons.

Schramm and Fiset [16] suggest that a small fraction of the material at the neutron-closed shell $N = 184$ could climb along this closed shell during the freeze out of the r-process neutron flux and reach the superheavy island. However, as seen in Fig. 8, such nuclei would reach Cape Farewell [17] somewhere between $Z = 98$ and 102 and suffer neutron-induced fission before reaching the superheavy island.

4.2 Conventional nuclear explosions

Conventional nuclear explosions yield neutron exposures similar to those in the astrophysical r-process; however, the time duration is so short ($\Delta t \lesssim 10^{-6}$ sec) that there is no time for beta decays during the neutron-capture process. The thermal photon temperature is much less than that in the r-process. The neutron captures therefore proceed to a lower neutron separation energy, which extends into a more neutron-rich region. In nuclear explosions to date, targets of various actinide nuclei have been irradiated with intense neutron sources. Independent of the target used or the intensity of the neutron irradiation, the heaviest nucleus recovered from the debris has been ^{257}Fm [18].

We can understand this failure to produce heavier nuclei in terms of our results. From Fig. 8 we see that neutron-induced fission terminates the neutron-capture chain on the U isotopes at mass number A = 256. Actually, neutron-induced fission should occur somewhat before this because we overestimate the barrier for U isotopes in this region by 1 or 2 MeV by not including mass-asymmetric distortions. Thus, we conclude that conventional nuclear explosions have even less hope for producing superheavy nuclei than the r-process.

From Fig. 8 we see that if a lighter target (such as ^{227}Ac, ^{226}Ra, or ^{222}Rn) were used, the neutron capture could proceed well beyond A = 256. The results of Fig. 6 show that subsequent beta-decay products would have barriers lower than 4.5 MeV and would therefore spontaneously fission with short half-lives. We have not performed spontaneous-fission half-life calculations for these nuclei, but perhaps some odd-mass chains could survive spontaneous fission and produce nuclei that live long enough ($\gtrsim$6 h) to be detected in the debris. Neutron exposure experiments on targets of Ac, Ra, or Rn could yield valuable information about the spontaneous-fission half-lives in this region of nuclei. This broad region of nuclei with fission barriers lower than 4.5 MeV (referred to by Nilsson as the Bay of Pigs) is also found in the calculations of Boleu et al. [15].

4.3 Multistep process

The failure of conventional nuclear explosions to produce superheavy nuclei has led Meldner [5] to propose a multistep explosive process that would allow beta decays between subsequent explosions. However, his process seems fraught with the same difficulties encountered in the r-process and in conventional nuclear explosions. Certainly odd-mass capture chains would have to be utilized as well as a target lighter than Th to avoid initial termination of the process by neutron-induced fission. It would then be required that beta decay lead to a region of stability against neutron-induced fission before the next neutron burst.

Meldner would like to take advantage of neutron capture along odd-proton chains where the fission barrier could be enhanced relative to the barrier heights of even nuclei. In the actinide region the spontaneous-fission half-lives of odd-particle nuclei are systematically about 10^3 times as long as those of neighboring even nuclei [19]. These hindrances arise from an increase either in the height of the barrier or in the inertia (or in both). If this hindrance factor is assumed to arise only from an increase in the barrier height, then the barriers for odd-particle nuclei are raised by about 0.5 MeV relative to those for even nuclei [1].

An examination of Fig. 8 reveals that after an initial neutron burst and subsequent beta decay into the Bay of Pigs, the nuclei would be in a region where a second neutron burst would initiate neutron-induced fission. This conclusion also applies for odd-proton capture chains. We conclude therefore that the multistep process has little chance of reaching the superheavy island.

5. CONCLUSIONS

We have used an improved version of the macroscopic-microscopic method to calculate fission barriers and neutron separation energies for a broad region of heavy neutron-rich nuclei. On the basis of these calculations we conclude that neutron-induced fission terminates the three possible multiple-neutron-capture processes well before the superheavy island is reached. However, it is possible that the use of somewhat lighter targets in conventional nuclear explosions could lead to the production of slightly heavier nuclei than are obtained at present.

ACKNOWLEDGMENTS

We are grateful for stimulating discussions with G. A. Cowan, S. E. Koonin, H. W. Meldner, P. Möller, W. D. Myers, S. G. Nilsson, D. N. Schramm, P. A. Seeger, and A. J. Sierk.

REFERENCES

[1] MYERS, W. D., SWIATECKI, W. J., Nucl. Phys. 81 (1966) 1.

[2] NILSSON, S. G., TSANG, C. F., SOBICZEWSKI, A., SZYMAŃSKI, Z., WYCECH, S., GUSTAFSSON, C., LAMM, I. L., MÖLLER, P., NILSSON, B., Nucl. Phys. A131 (1969) 1.

[3] BOLSTERLI, M., FISET, E. O., NIX, J. R., NORTON, J. L., Phys. Rev. C 5 (1972) 1050.

[4] FISET, E. O., NIX, J. R., Nucl. Phys. A193 (1972) 647.

[5] MELDNER, H. W., Phys. Rev. Lett. 28 (1972) 975.

[6] MÖLLER, P., NIX, J. R., Paper IAEA-SM-174/202, these Proceedings.

[7] MYERS, W. D., SWIATECKI, W. J., Berkeley Preprint UCRL-19543 (1970).

[8] MYERS, W. D., SWIATECKI, W. J., unpublished work (1973).

[9] MYERS, W. D., Nucl. Phys. A145 (1970) 387.

[10] NIX, J. R., Nucl. Phys. A130 (1969) 241.

[11] SIERK, A. J., NIX, J. R., Paper IAEA-SM-174/74, these Proceedings.

[12] SEEGER, P. A., Atomic Masses and Fundamental Constants (Proc. Conf. Teddington, 1971), Plenum, London (1972) 255.

[13] MYERS, W. D., SWIATECKI, W. J., Ark. Fys. 36 (1967) 343.

[14] SEEGER, P. A., FOWLER, W. A., CLAYTON, D. D., Ap. J. Suppl. 11 (1965) 121.

[15] BOLEU, R., NILSSON, S. G., SHELINE, R. K., TAKAHASHI, K., Phys. Lett. 40B (1972) 517.

[16] SCHRAMM, D. N., FISET, E. O., Ap. J. 180 (1973) 551.

[17] NILSSON, S. G., private communication (1973).

[18] ECCLES, S. F., Symposium on Engineering with Nuclear Explosions (Proc. Symp. Las Vegas, 1970), CONF-700101, USAEC Division of Technical Information, Springfield (1970) 1269.

[19] HYDE, E. K., The Nuclear Properties of the Heavy Elements, Vol. III, Fission Phenomena, Prentice-Hall, Englewood Cliffs (1964) 50.

FIGURE CAPTIONS

Fig. 1. Plot of known and predicted nuclei as a function of neutron number N and proton number Z. The three possible ways to reach the island of superheavy nuclei by the multiple capture of neutrons are illustrated.

Fig. 2. Comparison of experimental and calculated ground-state single-particle corrections. The difference between the experimental and calculated values is given in the lower portion of the figure. The ground-state single-particle correction is the nuclear mass excess relative to the spherical droplet-model energy.

Fig. 3. Fission barriers for nuclei as functions of the distance between the mass centers of the nascent fragments. The dashed curves give the droplet-model contributions and the solid curves the total potential energies. These barriers are calculated by use of the y family of shapes out to the distortion y = 0.2 and the most probable liquid-drop-model dynamical path for fissility parameter x = 0.8 for larger distortions. The microscopic contributions to the barriers are calculated with the single-particle levels for ^{264}Fm.

Fig. 4. These barriers are calculated by use of the y family of shapes out to the distortion y = 0.1 and the most probable liquid-drop-model dynamical path for fissility parameter x = 0.9 for larger distortions. The microscopic contributions to the barriers are calculated with the single-particle levels for ^{284}Fm.

Fig. 5. These barriers are calculated by use of the most probable liquid-drop-model dynamical path for fissility parameter x = 1.0. The microscopic contributions to the barriers are calculated with the single-particle levels for ^{290}114.

Fig. 6. Contour plot of the calculated fission-barrier height as a function of neutron number N and proton number Z for even nuclei.

Fig. 7. Contour plot of the calculated neutron separation energy as a function of neutron number N and proton number Z for even nuclei.

Fig. 8. Contour plot of the difference between the fission barrier height and the neutron separation energy for even nuclei. When this difference is less than about 1 MeV, the capture of a neutron leads to immediate fission.

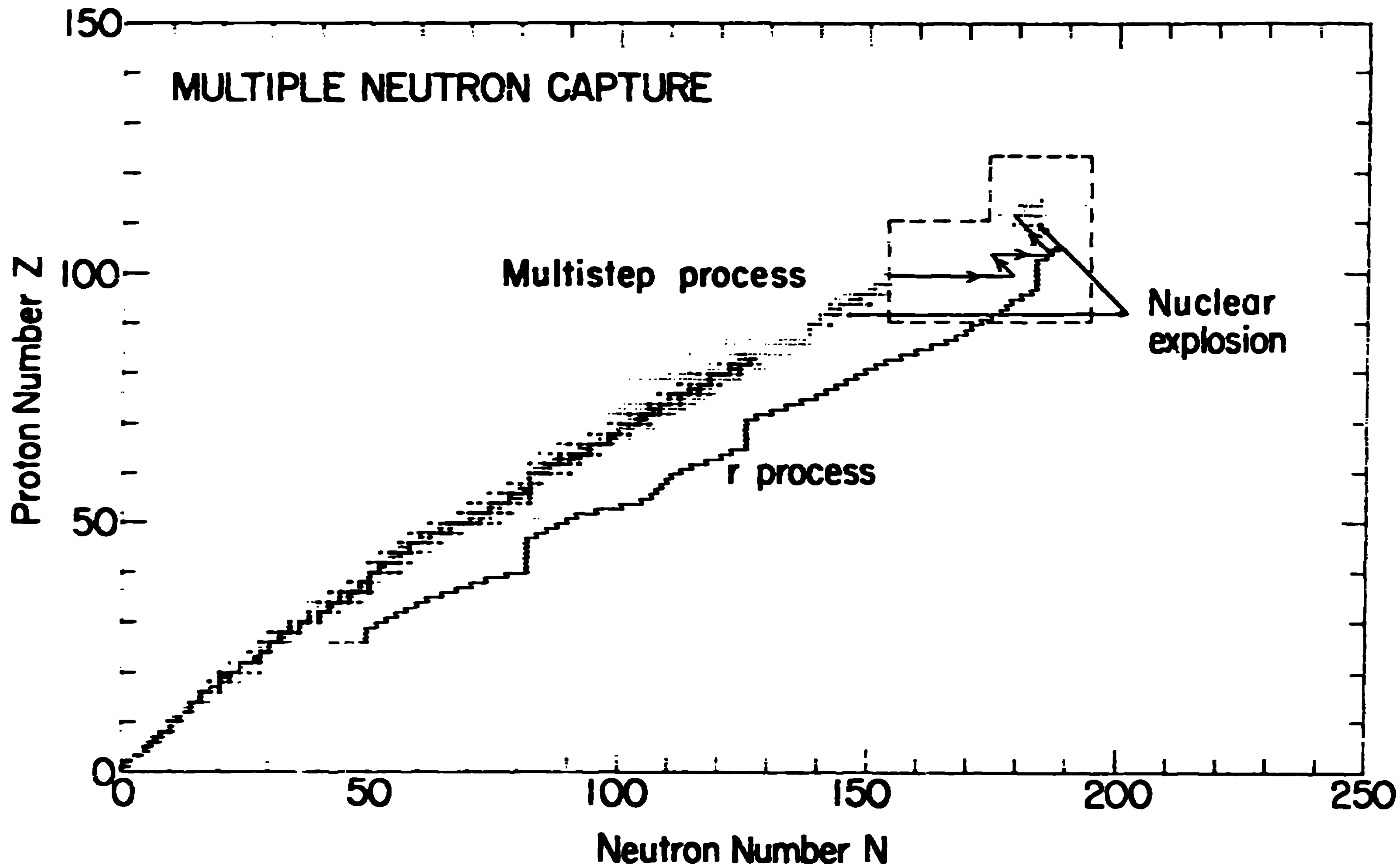
MULTIPLE NEUTRON CAPTURE
Multistep process
Nuclear explosion
r process
Proton Number Z
Neutron Number N
0
50
100
150
200
250
0
50
100
150

Fig. 1

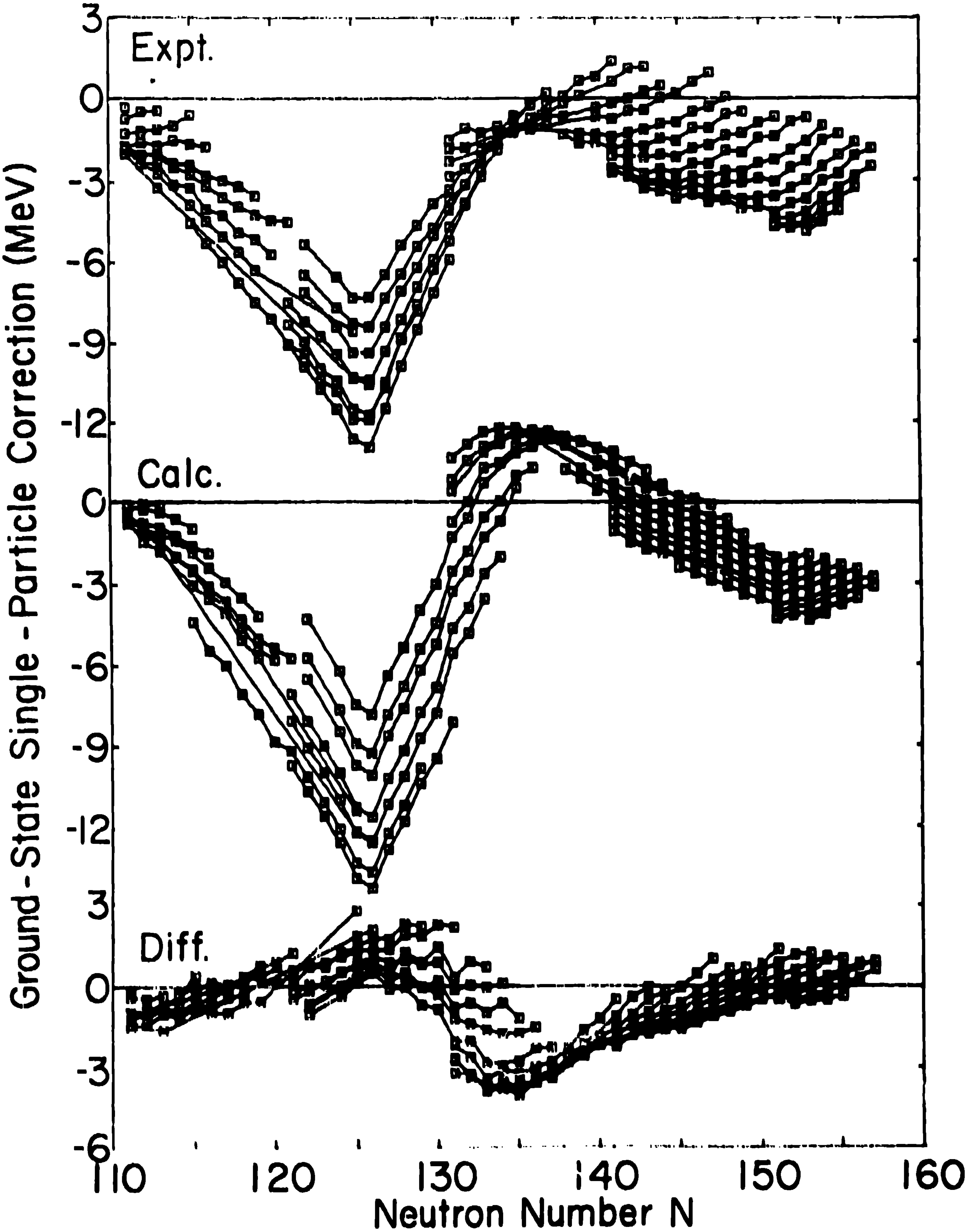
Expt.
Calc.
Diff.
Ground-State Single-Particle Correction (MeV)
3
0
-3
-6
-9
-12
-6
110
120
130
140
150
160
Neutron Number N

Fig. 2

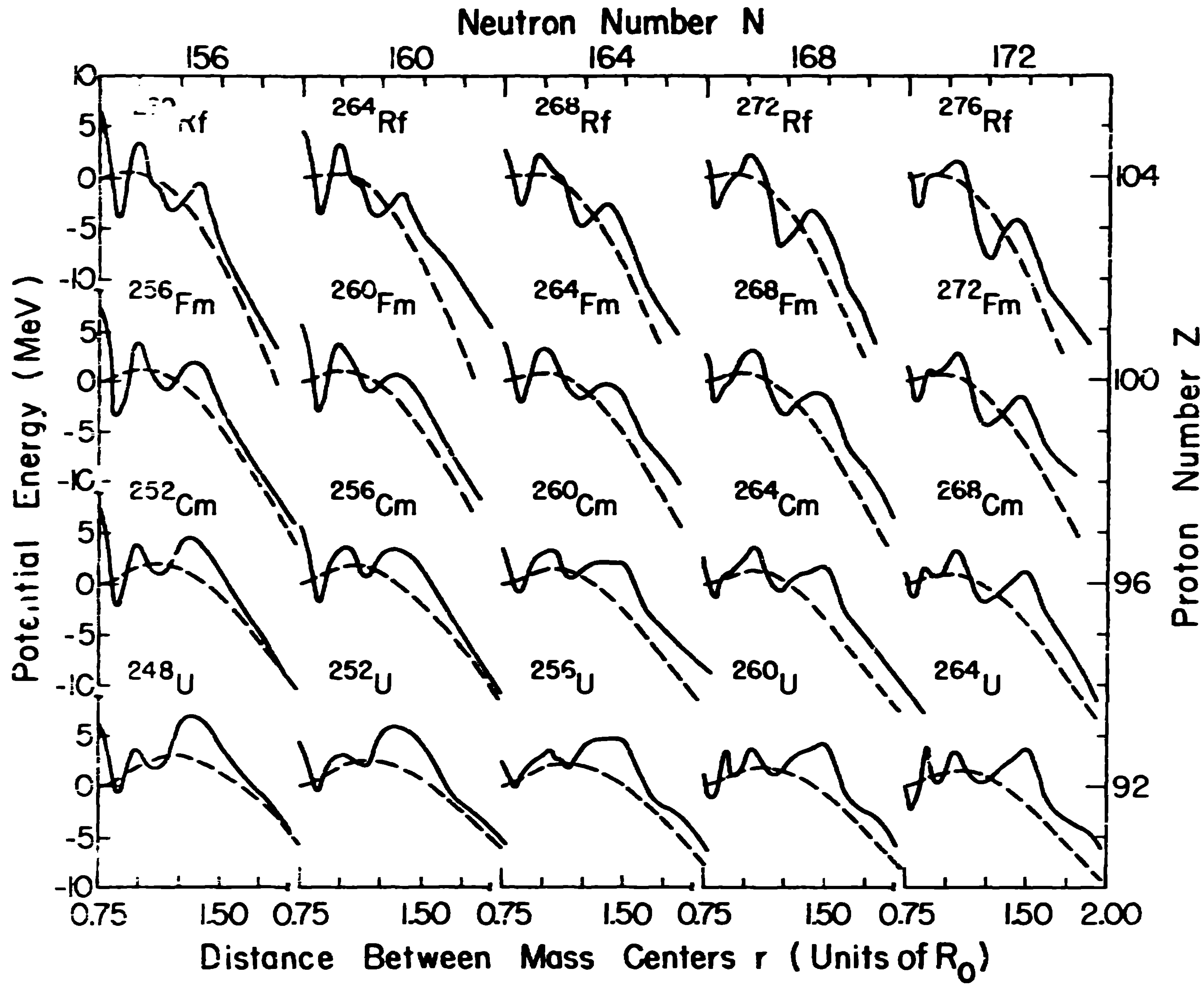
Neutron Number N
156
160
164
168
172
264Rf
268Rf
272Rf
276Rf
256Fm
260Fm
264Fm
268Fm
272Fm
252Cm
256Cm
260Cm
264Cm
268Cm
248U
252U
256U
260U
264U
Potential Energy (MeV)
Proton Number Z
104
100
96
92
0.75
1.50
2.00
Distance Between Mass Centers r (Units of R0)

Fig. 3

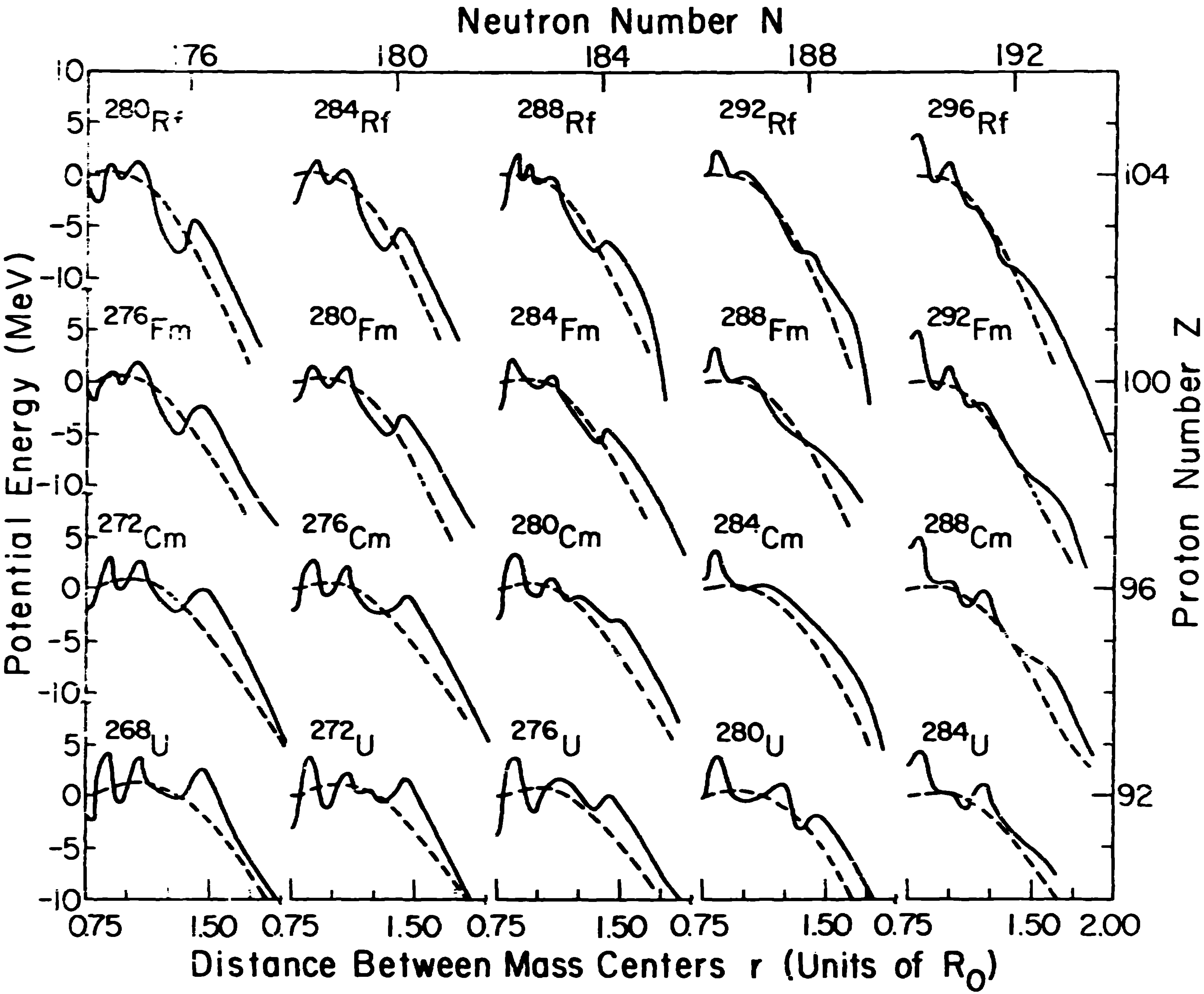
Neutron Number N
176
180
184
188
192
280Rf
284Rf
288Rf
292Rf
296Rf
276Fm
280Fm
284Fm
288Fm
292Fm
272Cm
276Cm
280Cm
284Cm
288Cm
268U
272U
276U
280U
284U
Potential Energy (MeV)
10
5
0
-5
-10
Proton Number Z
104
100
96
92
0.75
1.50
2.00
Distance Between Mass Centers r (Units of R_0)

Fig. 4

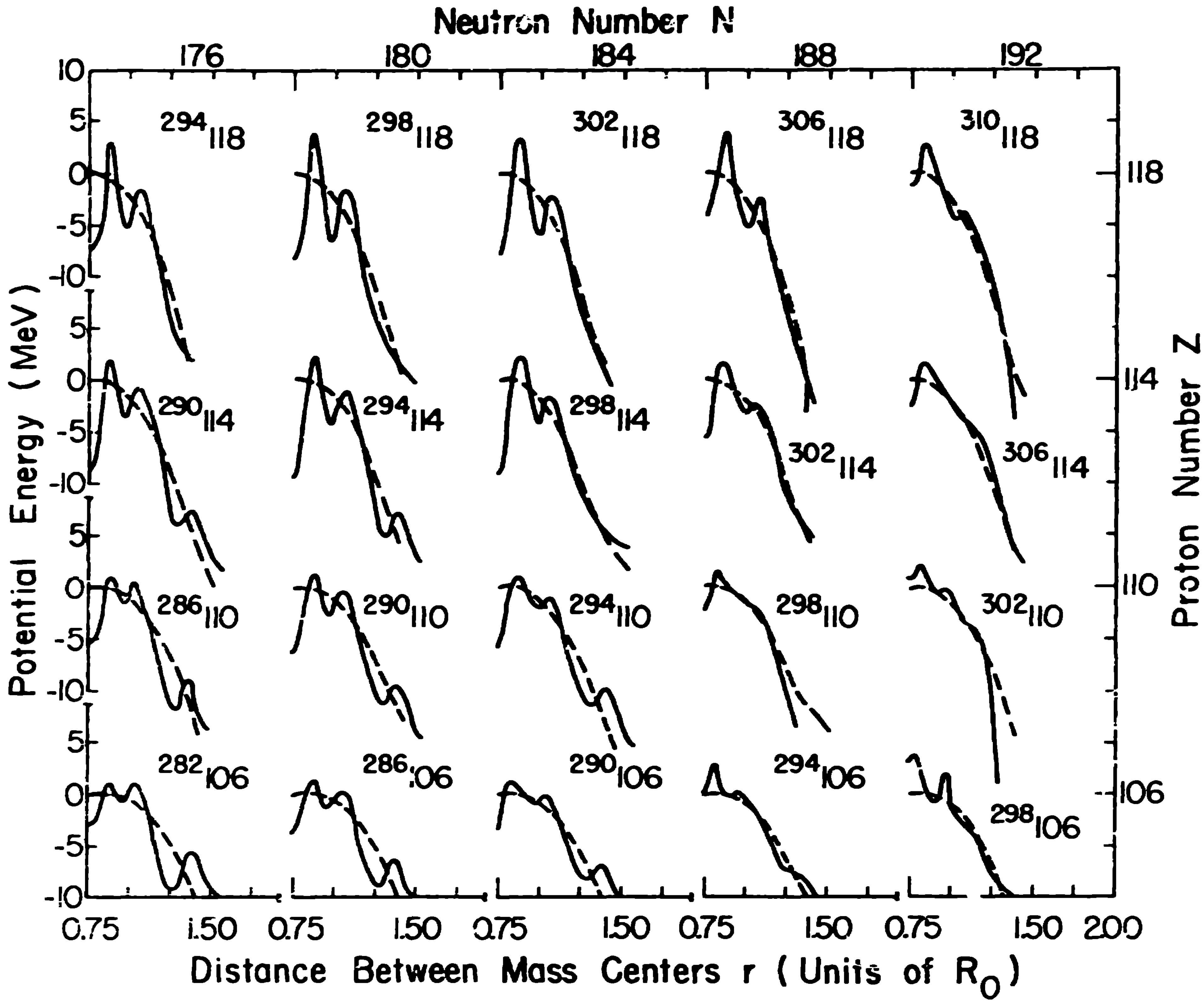
Neutron Number N
176
180
184
188
192
Potential Energy (MeV)
Proton Number Z
118
114
110
106
294 118
298 118
302 118
306 118
310 118
290 114
294 114
298 114
302 114
306 114
286 110
290 110
294 110
298 110
302 110
282 106
286 106
290 106
294 106
298 106
0.75
1.50
2.00
Distance Between Mass Centers r (Units of R0)

Fig. 5

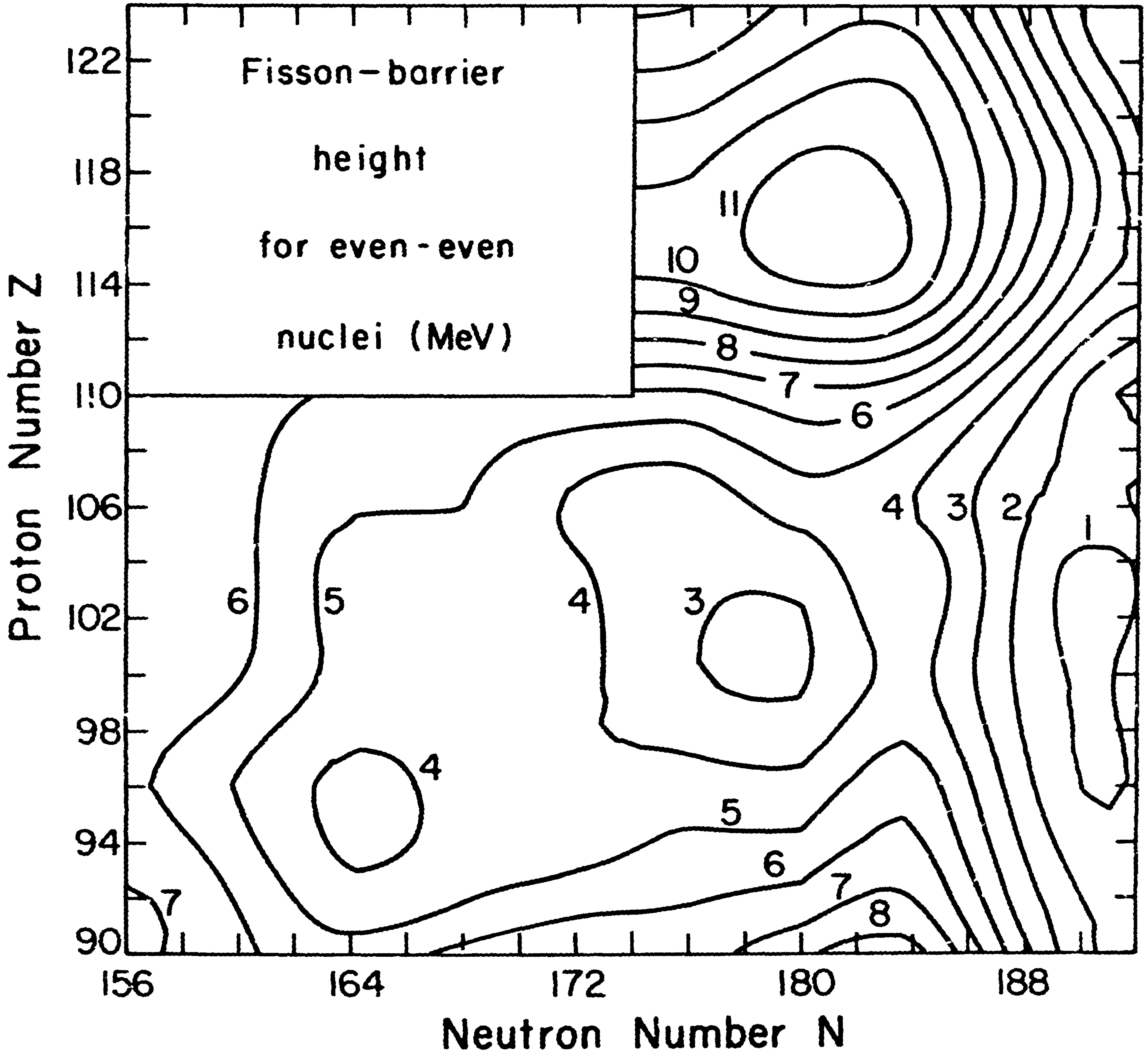
Fisson-barrier
height
for even-even
nuclei (MeV)
Proton Number Z
122
118
114
110
106
102
98
94
90
Neutron Number N
156
164
172
180
188
11
10
9
8
7
6
5
4
3
2
1

Fig. 6

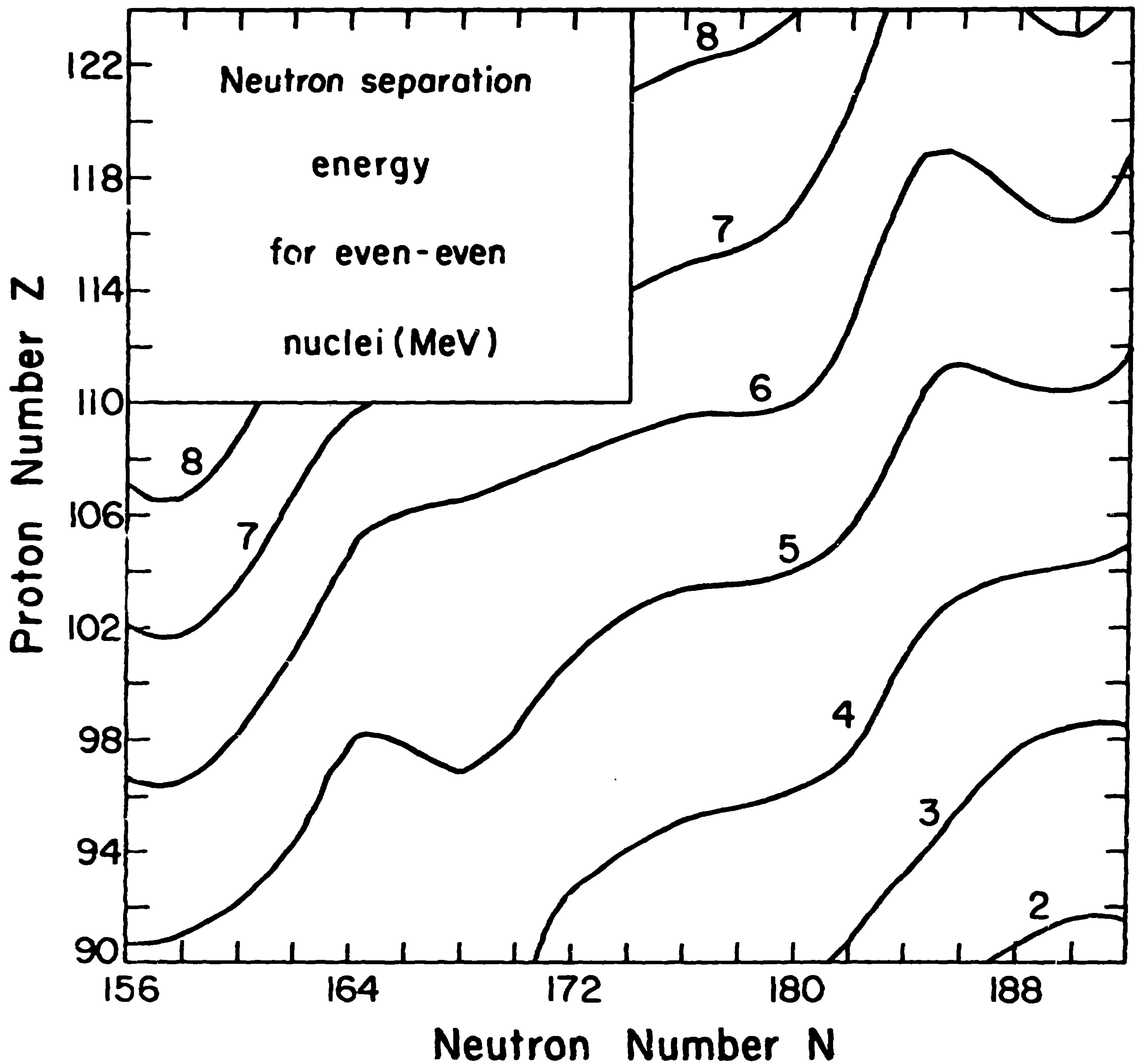
Neutron separation
energy
for even-even
nuclei (MeV)
Proton Number Z
Neutron Number N
90
94
98
102
106
110
114
118
122
156
164
172
180
188
2
3
4
5
6
7
8
7
8

Fig. 7

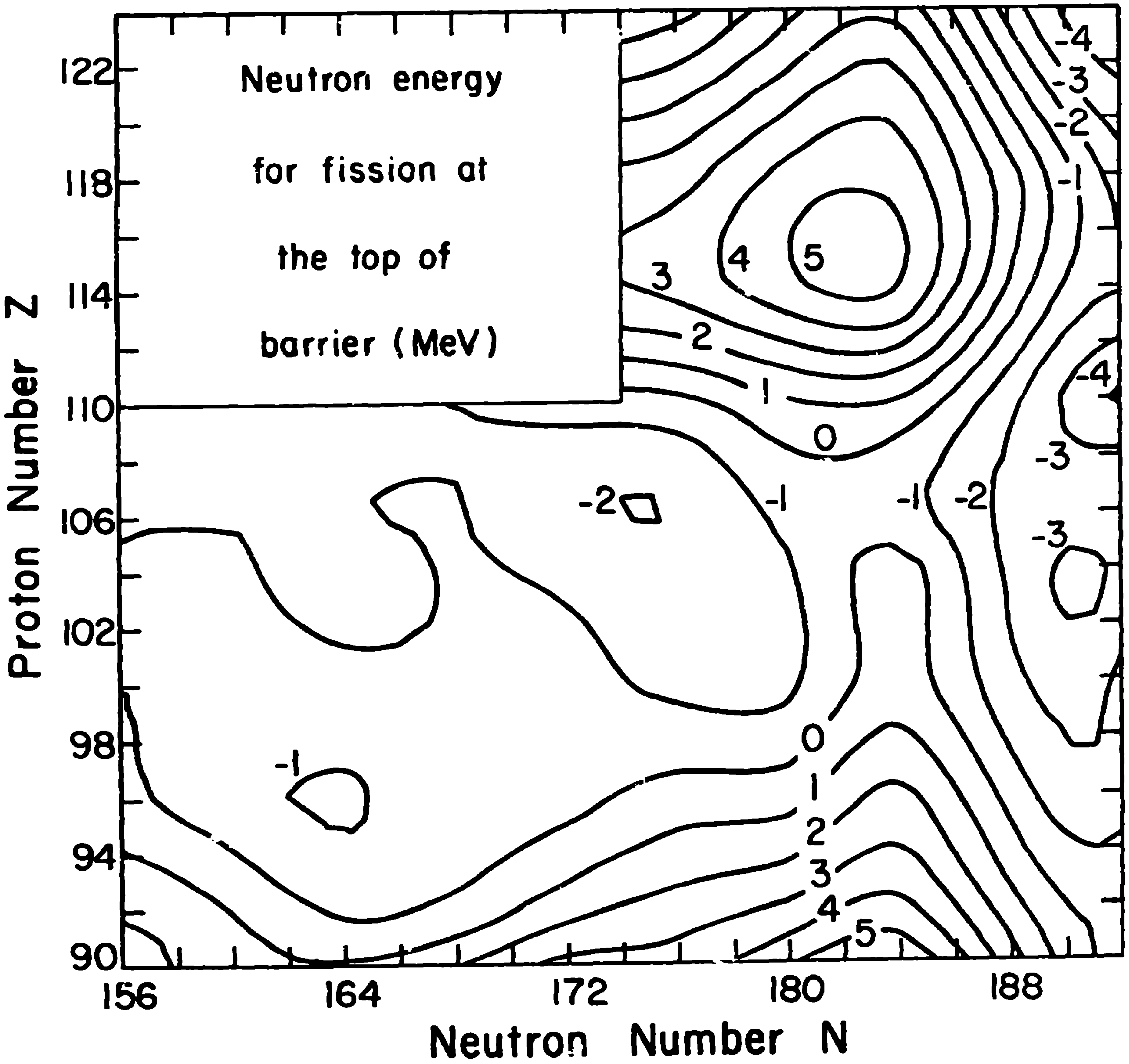
Neutron energy
for fission at
the top of
barrier (MeV)
Proton Number Z
Neutron Number N
122
118
114
110
106
102
98
94
90
156
164
172
180
188
5
4
3
2
1
0
-1
-2
-3
-4

Fig. 8